Proceedings of ERAD 2006

Influence of non-uniform radar beam filling on attenuation correction at C- and X-band

Alexis Berne[1] **and Remko Uijlenhoet**[2]

[1]Laboratoire d'étude des Transferts en Hydrologie et Environnement, Grenoble (France).
[2]Hydrology and Quantitative Water Management Group, Wageningen University (The Netherlands).

1 Introduction

At short wavelengths, the attenuation of the radar signal due to precipitation along its path constitutes a major source of error for radar rainfall estimation. The different techniques developed to correct for this attenuation generally assume that the radar sampling volumes are homogeneously filled by rainfall. However, rainfall is highly variable over a large range of scales, and the influence of the heterogeneity within the radar sampling volume, also known as non-uniform beam filling (NUBF), needs to be quantified.

A recently developed stochastic simulator of range profiles of raindrop size distributions (DSD) provides a controlled experiment framework to quantitatively investigate the influence of NUBF on attenuation correction. Using a Monte Carlo approach, we generate 1000 profiles of 30 km long, with an initial resolution of 25 m. By averaging the profiles, the resolution is progressively decreased to 5 km. Two attenuation correction algorithms are applied to the generated attenuated profiles, and the evolution of their performance with the decreasing resolution is quantified. In this work, we focus on incoherent non-polarimetric single-frequency ground-based radar systems, and NUBF only concerns the radial heterogeneity within the radar sampling volume.

Section 2 is devoted to the description of the DSD simulator. In Section 3, the two attenuation correction algorithms are presented. The results are described and commented in Section 4.

2 DSD simulator

The range profiles of DSDs have been generated using the stochastic simulator proposed by Berne and Uijlenhoet (2005). It is based on an exponential DSD model:

$$N(D|N_t,\lambda) = N_t\,\lambda\,e^{-\lambda D}\ , \tag{1}$$

where $N(D|N_t,\lambda)dD$ denotes the drop concentration in the diameter interval [D,D+dD] given N_t (drop concentration in m^{-3}) and λ (in mm^{-1}). The two parameters N_t and λ are assumed to be random variables, jointly lognormally distributed. To introduce a spatial structure in the profiles, $N' = \ln N_t$ and $\lambda' = \ln \lambda$ are assumed to follow a first order discrete vector auto-regressive process. This results in an exponential auto-correlation function:

$$\rho(r) = e^{-2r/\theta}\ , \tag{2}$$

where r represents the distance lag and θ the characteristic spatial scale, also known as the scale of fluctuation:

$$\theta = 2\int_0^{+\infty}\rho(r)\,dr\ . \tag{3}$$

The stochastic simulator is able to produce ensembles of range profiles of DSDs of equivolumetric spherical drops.

DSD time series measurements from an optical spectro-pluviometer, collected during the HIRE'98 experiment in Marseille, France, are used to parameterize the simulator. A set of parameters is derived from a 45-min period of intense rainfall (about 60 mm h^{-1} on average) during the 7 September 1998 rain event, and corresponds to convective rainfall. Assuming Taylor's hypothesis with a constant velocity of 12.5 m s^{-1}, the required spatial characteristics of N' and λ' are derived. To achieve a high spatial resolution of 25 m, DSD data have been analyzed at a 2-s time step. The length of the profiles is fixed to 30 km. The analysis of the fitted N' and λ' values shows that the cross-correlation can be considered as negligible. The number of model parameters now reduces to five: the mean and standard deviation of

Correspondence to: Alexis Berne
(Alexis.Berne@hmg.inpg.fr)

Table 1. Mean, standard deviation and characteristic spatial scale of $N' = \ln N_t$ and $\Lambda' = \ln \lambda$ deduced from HIRE'98 data (45-min intense rainfall period during the 07/09/1998 event) at a 2-s time step.

	Mean	Std	θ (km)
N'	8.11	0.41	4.4
λ'	0.93	0.31	4.4

N' and λ', and the characteristic scale θ (assumed to be equal for N' and λ'). Their values are given in Table 1.

A total number of 1000 profiles of DSD parameters have been generated, and the corresponding profiles of (one-way) specific attenuation k and rain rate R have been computed, using the Mie theory for the scattering cross-sections (van de Hulst, 1981) and Beard's velocity model for the drop terminal fall velocity (Beard, 1977). The specific attenuation (in dB km^{-1}) is defined as

$$k = \frac{1}{\ln 10} \int_0^\infty \sigma_E(D) N(D|N_t, \lambda)\, dD \tag{4}$$

where σ_E [cm^2] is the extinction cross-section. Similarly, the rain rate (in mm h^{-1}) is defined as

$$R = 6\pi\, 10^{-4} \int_0^\infty D^3 v(D) N(D|N_t, \lambda)\, dD \tag{5}$$

where $v(D)$ denotes the terminal fall speed (in m s^{-1}) of a drop of diameter D. Fig. 1 shows an example of generated profile of rain rate R, of radar reflectivity Z and the corresponding attenuated reflectivity Z_a, at a wavelength of 3.2 cm (X-band). This controlled experiment framework allows to adopt a Monte Carlo approach to quantitatively investigate the influence of NUBF on the attenuation correction accuracy and robustness.

3 Attenuation correction algorithms

As mentioned in the introduction, we consider incoherent, single frequency and non-polarimetric radar systems. Two different types of algorithms will be studied in the following. The first attenuation correction algorithm corresponds to a forward implementation and is based on the analytical solution proposed by Hitschfeld and Bordan (1954). The second algorithm corresponds to a backward implementation and is based on the analytical solution proposed by Marzoug and Amayenc (1994).

The measured attenuated reflectivity Z_a reads (assuming there is no calibration error)

$$Z_a(r) = A(r) Z(r)\ , \tag{6}$$

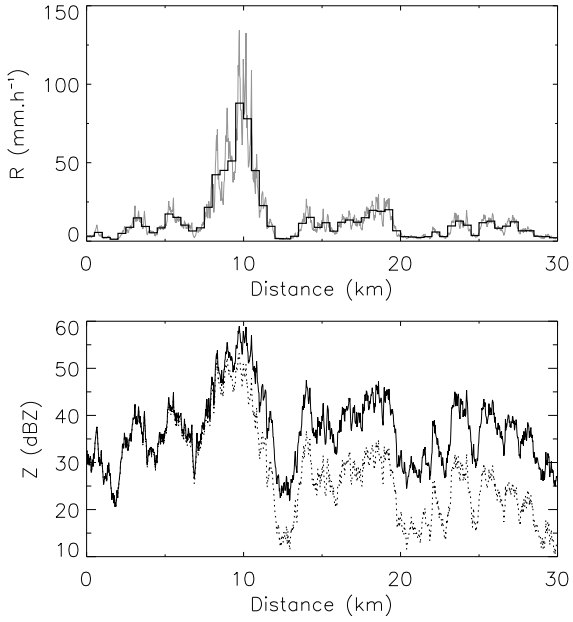

Fig. 1. Example of generated profile of rain rate R and the corresponding attenuated Z_a (dotted line) and non-attenuated Z (solid line) profiles at X-band, at 25 and 500-m resolution.

where $A(r)$ is the two-way attenuation factor at the range r ($0 \leq A \leq 1$). Assuming the Z-k relation reads

$$Z = \alpha\, k^\beta\ , \tag{7}$$

A can be written as

$$A(r) = \exp\left[-0.2 \ln(10) \int_0^r \left(\frac{Z(s)}{\alpha}\right)^{1/\beta} ds\right]\ . \tag{8}$$

Hitschfeld and Bordan (1954) (HB hereafter) proposed an analytical solution to express Z as a function of Z_a:

$$Z(r) = Z_a(r) \Big/ \left[1 - \frac{0.2 \ln(10)}{\beta} \int_0^r \left(\frac{Z_a(s)}{\alpha}\right)^{1/\beta} ds\right]^\beta\ . \tag{9}$$

The HB algorithm is a forward algorithm because the integral is between 0 and r. However, the difference in its denominator can be close to 0 and this makes the algorithm potentially highly unstable (Hitschfeld and Bordan, 1954).

To avoid instability problems, another family of attenuation correction algorithms has been developed. It is based on the knowledge of an estimate A_0 of the PIA at a given range r_0. For ground based radar, ground echoes may be used to derive PIA estimates by comparing their reflectivity values during dry and rainy periods, as proposed by Delrieu et al. (1997). The reformulation of Eq.(9) starting from r_0 and going backward to the radar guarantees the stability of

the algorithms. As an example, we use the solution proposed by Marzoug and Amayenc (1994) (MA hereafter):

$$Z(r) = Z_a(r) \Big/ \left[A_0^{1/\beta} + \frac{0.2\ln(10)}{\beta} \int_r^{r_0} \left(\frac{Z_a(s)}{\alpha} \right)^{1/\beta} ds \right]^{\beta}. \quad (10)$$

The main drawback of such a backward algorithm is that it requires a reliable estimation of the PIA at a given range.

4 Quantification of the influence of NUBF on attenuation correction

The 1000 profiles are averaged at 50, 125, 250, 500, 1000, 1500, 2000 and 2500-m resolutions. This set of consistent profiles at different resolutions enables us to quantitatively investigate the influence of NUBF on the uncertainty of attenuation correction using the two algorithms described previously.

To quantify the error in the corrected Z profiles, we use the root mean square error (RMSE) and the mean bias error (MBE, defined as a ratio) calculated with respect to the true Z profiles. Figure 3 presents the median value of these two criteria over the 1000 profiles, as a function of the resolution (normalized by the characteristic scale of rainfall) and of the PIA, at X-band (3.2 cm). Figure 4 is similar to Figure 3, but for C-band (5.6 cm). These two figures show that the influence of NUBF is limited for the two algorithms when the resolution is higher than about 20% of the characteristic scale of rainfall, at X- and C-band. Both algorithms tend to underestimate (MBE values lower than 1), as already shown in previous work (e.g. Gosset and Zawadzki, 2001).

For the HB algorithm, the error due to NUBF is small in comparison with the error due to rainfall variability between the different radar sampling volumes along the profile. Moreover, as illustrated in Figure 2, the number of diverging profiles reduces when the resolution becomes coarser.

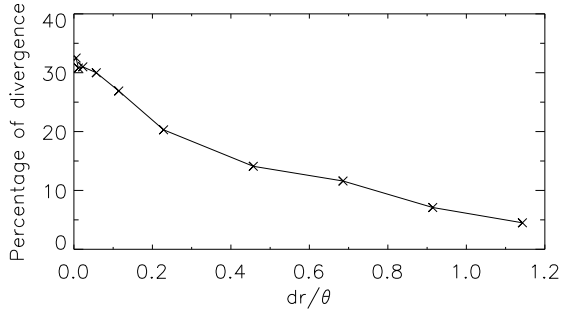

Fig. 2. Percentage of diverging retrieved reflectivity profiles for the HB algorithm as a function of the resolution, normalized by the characteristic scale of rainfall, at X-band.

On the other hand, the MA algorithm appears more sensitive to NUBF, especially for coarse resolutions and large PIA values. Nevertheless, the error associated with the MA algorithm remains about one order of magnitude lower than that associated with the HB algorithm. It must be noted that this corresponds to an ideal case with no other sources of error than NUBF.

5 Conclusions

Attenuation is a major source of error for rainfall estimation at short wavelengths (e.g., C- and X-band). Classical attenuation correction algorithms for incoherent non-polarimetric single-frequency weather radar systems assume a power law between the radar reflectivity Z and the specific attenuation k. However, this relation is not linear, and the influence of NUBF on the performance of such algorithms is investigated in the present work.

Within a simulation framework based on a DSD profile generator, the influence of NUBF on the uncertainty associated with the HB algorithm (Hitschfeld and Bordan, 1954) and the MA algorithm (Marzoug and Amayenc, 1994) is quantified. It appears limited for both algorithms when the radial resolution of the radar sampling volume is higher than 20% of the characteristic scale of rainfall. NUBF has a stronger influence on the MA algorithm, which nevertheless remains more accurate than the HB algorithm.

Acknowledgements. EU Integrated project FLOODsite (contract GOCE-CT-2004-505420) and NWO (grant 016.021.003).

References

Beard, K.: Terminal velocity adjustment for cloud and precipitation drops aloft, J. Atmos. Sci., 34, 1293–1298, 1977.

Berne, A. and Uijlenhoet, R.: A stochastic model of range profiles of raindrop size distributions: application to radar attenuation correction, Geophys. Res. Lett., 32, L10803, doi:10.1029/2004GL021899, 2005.

Delrieu, G., Caoudal, S., and Creutin, J.-D.: Feasibility of using mountain return for the correction of ground-based X-band weather radar data, J. Atmos. Oceanic Technol., 14, 368–385, 1997.

Gosset, M. and Zawadzki, I.: Effect of nonuniform beam filling on the propagation of the radar signal at X-band frequencies. Part I: changes in the *k(Z)* relationship, J. Atmos. Oceanic Technol., 18, 1113–1126, 2001.

Hitschfeld, W. and Bordan, J.: Errors inherent in the radar measurement of rainfall at attenuating wavelengths, J. Meteor., 11, 58–67, 1954.

Marzoug, M. and Amayenc, P.: A class of single- and dual-frequency algorithms for rain-rate profiling from a spaceborne radar. Part I: principle and tests from numerical simulations, J. Atmos. Oceanic Technol., 11, 1480–1506, 1994.

van de Hulst, H.: Light scattering by small particles, Dover, 1981.

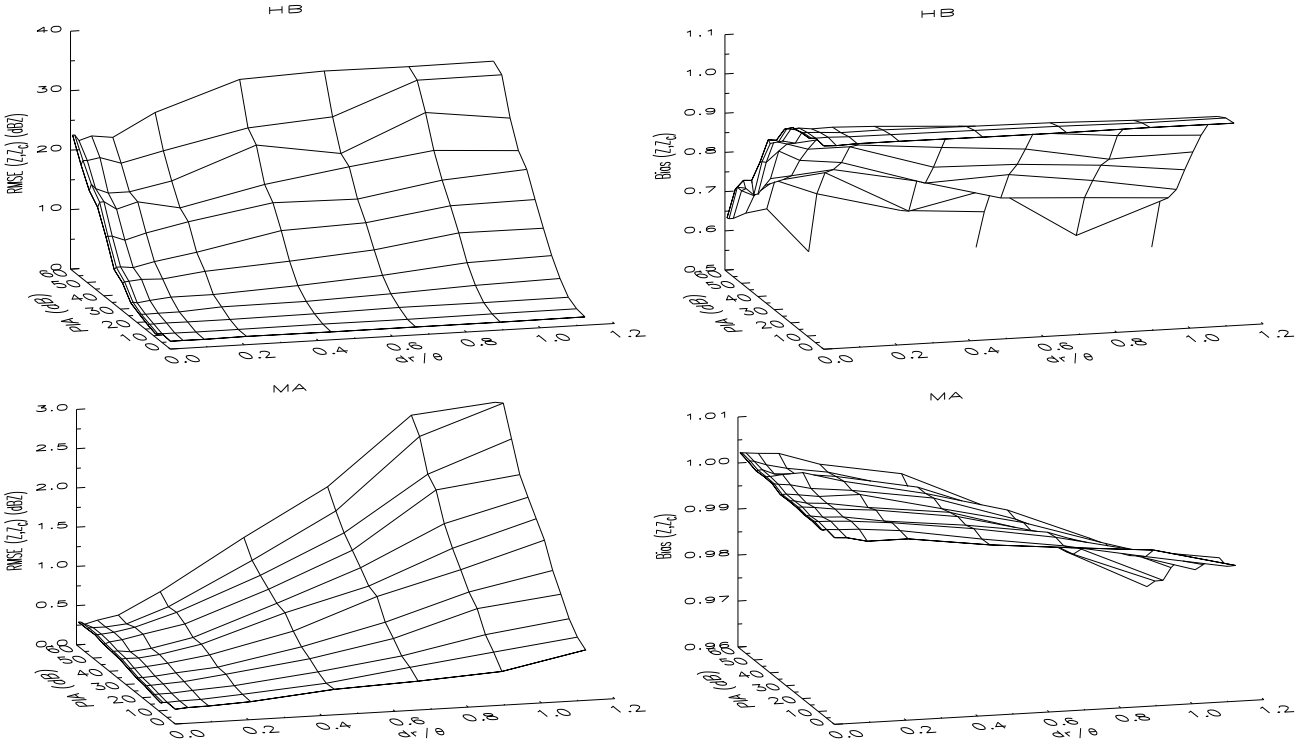

Fig. 3. RMSE (left pannels) and MBE (right pannels) as a function of resolution (normalized by the characteristic scale of rainfall) and of PIA, at X-band.

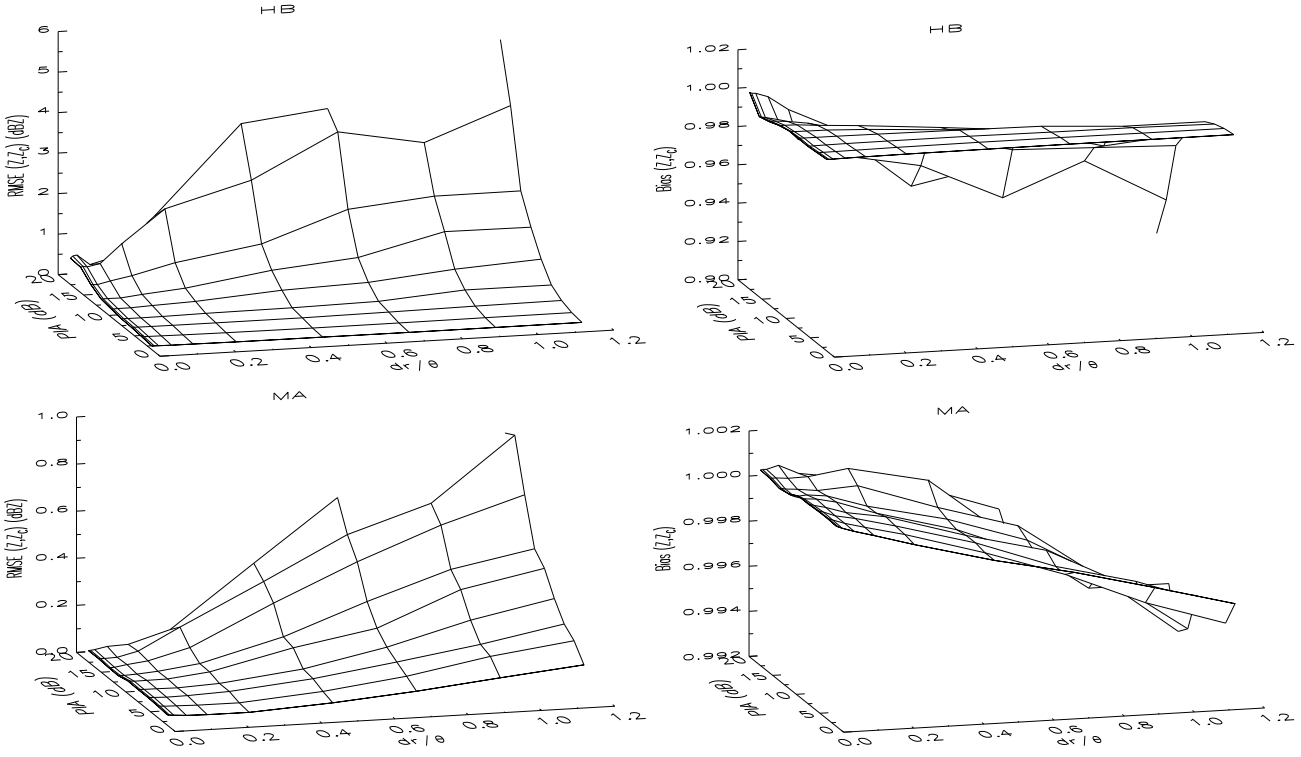

Fig. 4. RMSE (left pannels) and MBE (right pannels) as a function of resolution (normalized by the characteristic scale of rainfall) and of PIA, at C-band.